

# Receptor and viral determinants of SARS-coronavirus adaptation to human ACE2

Wenhui Li<sup>1</sup>, Chengsheng Zhang<sup>2,3</sup>, Jianhua Sui<sup>4</sup>, Jens H Kuhn<sup>1,5</sup>, Michael J Moore<sup>1</sup>, Shiwen Luo<sup>3</sup>, Swee-Kee Wong<sup>1</sup>, I-Chueh Huang<sup>1</sup>, Keming Xu<sup>3</sup>, Natalya Vasilieva<sup>6</sup>, Akikazu Murakami<sup>4</sup>, Yaqing He<sup>7</sup>, Wayne A Marasco<sup>4</sup>, Yi Guan<sup>3,\*</sup>, Hyeryun Choe<sup>6,\*</sup> and Michael Farzan<sup>1,\*</sup>

<sup>1</sup>Department of Microbiology and Molecular Genetics, Harvard Medical School, New England Primate Research Center, Southborough, MA, USA, <sup>2</sup>Department of Pathology and Molecular Medicine, McMaster University, Hamilton, Ontario, Canada, <sup>3</sup>Department of Microbiology, Queen Mary Hospital, The University of Hong Kong, Hong Kong SAR, PRC, <sup>4</sup>Department of Medicine, Dana-Farber Cancer Institute, Harvard Medical School, Boston, MA, USA, <sup>5</sup>Department of Biology, Chemistry, Pharmacy, Freie Universität Berlin, Berlin, Germany, <sup>6</sup>Department of Pediatrics, Children's Hospital, Harvard Medical School, Boston, MA, USA and <sup>7</sup>Center for Disease Control and Prevention of Shenzhen, Shenzhen, Guangdong Province, PRC

**Human angiotensin-converting enzyme 2 (ACE2) is a functional receptor for SARS coronavirus (SARS-CoV). Here we identify the SARS-CoV spike (S)-protein-binding site on ACE2. We also compare S proteins of SARS-CoV isolated during the 2002–2003 SARS outbreak and during the much less severe 2003–2004 outbreak, and from palm civets, a possible source of SARS-CoV found in humans. All three S proteins bound to and utilized palm-civet ACE2 efficiently, but the latter two S proteins utilized human ACE2 markedly less efficiently than did the S protein obtained during the earlier human outbreak. The lower affinity of these S proteins could be complemented by altering specific residues within the S-protein-binding site of human ACE2 to those of civet ACE2, or by altering S-protein residues 479 and 487 to residues conserved during the 2002–2003 outbreak. Collectively, these data describe molecular interactions important to the adaptation of SARS-CoV to human cells, and provide insight into the severity of the 2002–2003 SARS epidemic.**

*The EMBO Journal* (2005) **24**, 1634–1643. doi:10.1038/sj.emboj.7600640; Published online 24 March 2005

**Subject Categories:** microbiology & pathogens; molecular biology of disease

**Keywords:** angiotensin-converting enzyme 2; coronavirus; severe acute respiratory syndrome; viral adaptation

\*Corresponding authors. Y Guan, Department of Microbiology, Queen Mary Hospital, The University of Hong Kong, Hong Kong SAR, PRC. E-mail: yguan@hkucc.hku.hk or H Choe, Department of Pediatrics, Children's Hospital, Harvard Medical School, Boston, MA 02115, USA. E-mail: hyeryun.choe@tch.harvard.edu or M Farzan, Department of Microbiology and Molecular Genetics, Harvard Medical School, New England Primate Research Center, Southborough, MA 01772-9102, USA. Tel.: +1 617 768 8372; Fax: +1 617 768 8738; E-mail: farzan@hms.harvard.edu

Received: 9 December 2004; accepted: 4 March 2005; published online: 24 March 2005

## Introduction

SARS coronavirus (SARS-CoV) is the etiological agent of severe acute respiratory syndrome (SARS), an acute pulmonary syndrome that, when it emerged in the winter of 2002–2003, resulted in the death of approximately 800 individuals, close to 10% of those infected (Drosten *et al*, 2003; Fouchier *et al*, 2003; Ksiazek *et al*, 2003; Kuiken *et al*, 2003). Despite concerns that SARS-CoV would re-emerge, last winter (2003–2004), only a handful of individuals were found infected by the virus. These individuals appeared to have much less severe symptoms, and no secondary transmission was observed (Liang *et al*, 2004; Peiris *et al*, 2004; Song *et al*, 2005). Severe cases of SARS were also reported in 2004, but these resulted from laboratory infections (Normile, 2004).

The coronavirus spike (S) protein mediates infection of receptor-bearing cells (Gallagher and Buchmeier, 2001; Holmes, 2003; Hofmann and Pohlmann, 2004). Angiotensin-converting enzyme 2 (ACE2) is a functional receptor for SARS-CoV, and binds the SARS-CoV S protein with high affinity (Li *et al*, 2003). Several lines of evidence suggest that ACE2 is a physiologically relevant receptor during infection. Tissue expression of the receptor corresponds to the localization of virus in infected individuals and animals (Harmer *et al*, 2002; Chan *et al*, 2004; Ding *et al*, 2004; Hamming *et al*, 2004). Also, the efficiency of infection in humans, mice, and rats correlates with the ability of the ACE2 of each species to support viral replication (Li *et al*, 2004; Subbarao *et al*, 2004; Wentworth *et al*, 2004). Antibodies that block ACE2 association (Sui *et al*, 2004) protect mice against infection (Sui *et al*, 2005). Finally, although many cell lines do not express ACE2, most cell lines shown to support SARS-CoV infection or replication detectably express this receptor (Hofmann *et al*, 2004; Nie *et al*, 2004). Although DC-SIGNR (L-SIGN, CD209L) and DC-SIGN (CD209) have recently been shown to enhance infection of ACE2-expressing cells (Jeffers *et al*, 2004; Marzi *et al*, 2004; Yang *et al*, 2004), these proteins do not appear to mediate efficient infection in the absence of ACE2 (Jeffers *et al*, 2004; Marzi *et al*, 2004).

Unlike many type I fusion proteins, including those of other coronaviruses, the S protein of SARS-CoV is not cleaved in the virus-producing cell (Xiao *et al*, 2003; Moore *et al*, 2004). However, two domains corresponding to the S1 and S2 proteins of processed coronaviruses can be defined (Gallagher and Buchmeier, 2001). The S1 domain mediates receptor association, whereas the S2 domain is membrane-associated and likely undergoes structural rearrangements that mediate membrane fusion. A discrete receptor-binding domain (RBD) of the S protein has been defined at residues 318–510 of the S1 domain (Xiao *et al*, 2003; Babcock *et al*, 2004; Wong *et al*, 2004). This RBD binds ACE2 with higher affinity than does the full S1 domain (Wong *et al*, 2004).

Early cases of SARS in 2002 were reported to have occurred in animal traders and restaurant workers handling wild mammals, and SARS-CoV has been isolated from two such

mammals, palm civets (*Paguma larvata*) and raccoon dogs (*Nyctereutes procyonoides*) (Guan *et al*, 2003). Palm civets have also been implicated in the minor 2003–2004 SARS outbreak (Zhong, 2004). The sequences of the S-protein genes of 13 viruses isolated from palm civets, and one from raccoon dogs, have been determined (Guan *et al*, 2003; Song *et al*, 2005). Interestingly, the RBDs of these animal S proteins are highly conserved except residue 479, which varies between asparagine and basic amino acids, but differ at several positions from the RBDs of viruses isolated during the 2002–2003 outbreak. Although different from palm-civet-derived RBDs, the latter RBDs were themselves highly conserved in the more than 100 S-protein genes obtained during the severe human outbreak (He *et al*, 2004; Zhang *et al*, 2004). Full sequence has also been published for two S-protein genes obtained during the mild 2003–2004 outbreak (He *et al*, 2004; Song *et al*, 2005). These genes are nearly identical and contain elements common to S protein isolated during the earlier human outbreak and to that isolated from palm civets.

Here we describe the S-protein-binding domain of human ACE2 by characterizing chimeras of human and rat ACE2. By introducing four residues of human ACE2 into rat ACE2, we convert this receptor, which supports little or no S-protein-mediated infection, into a receptor that binds the S1 domain and supports infection, with efficiency close to that of human ACE2. By characterizing additional ACE2 variants, we localize the S-protein-binding domain primarily to  $\alpha$ -helix 1 of ACE2 and to a loop leading to  $\beta$ -sheet 5. We then show that a representative S protein from the mild 2003–2004 outbreak, and one from palm civets, mediates more efficient infection of cells expressing palm-civet ACE2 compared to cells expressing human receptor. In contrast, S protein from the severe 2002–2003 outbreak efficiently binds and utilizes both receptors. Two regions of the S-protein-binding site on ACE2, and two residues in the RBD of these S proteins, largely determine these differences. Our data describe S-protein adaptations, and their receptor counterparts, that permit efficient infection of human cells. These adaptations, absolutely conserved during 2002–2003 outbreak, may in part account for the unusual severity of SARS.

## Results

### Localization of the S-protein-binding domain on human ACE2

We have previously shown that S-protein-mediated infection of cells expressing human ACE2 is substantially more efficient than that of cells expressing the same levels of rat ACE2 (Li *et al*, 2004). We first investigated whether this difference localized to the ACE2 enzymatic or collectrin domain. The latter domain is defined by its close homology with a small, kidney-expressed protein of the same name (Zhang *et al*, 2001). Figure 1A shows that a fusion protein comprising the SARS-CoV S1 domain and the Fc domain of human IgG1 (S1-Ig) efficiently precipitated human ACE2, as well as an ACE2 chimera with the human catalytic domain and the rat collectrin domain. In contrast, S1-Ig could not precipitate rat ACE2 or an ACE2 chimera with the rat catalytic domain and the human collectrin domain. The ability of these chimeric receptors to bind S1-Ig was also reflected in their ability to support S-protein-mediated infection (Figure 2C). These data indicate that differences in the ability of rat and human ACE2

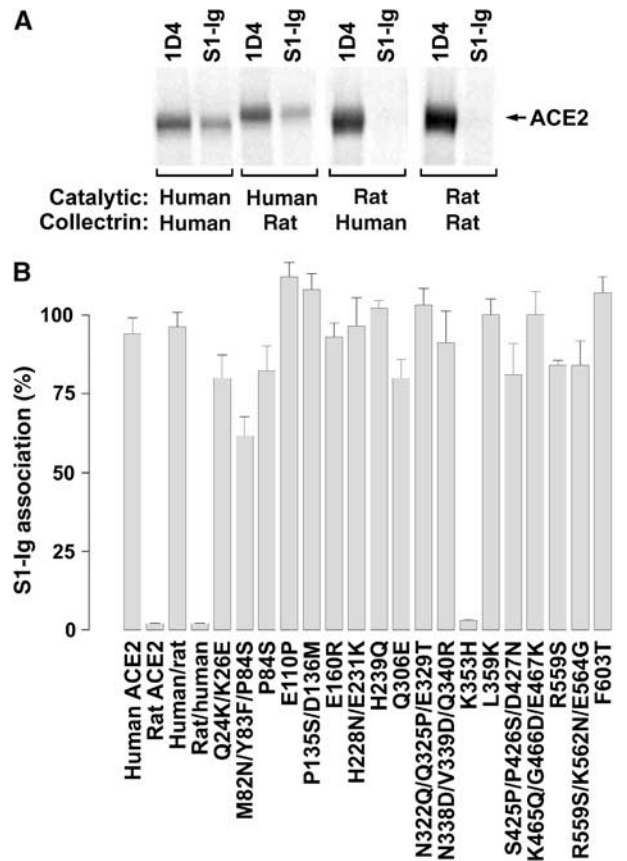


**Figure 1** Introduction of rat ACE2 residues into the human ACE2 catalytic domain interferes with S-protein association. (A) HEK293T cells were transfected with plasmids encoding human or rat ACE2, or chimeras of these receptors in which residues 1–600, corresponding to the ACE2 catalytic domain, were exchanged. Transfected cells were metabolically labeled with [<sup>35</sup>S]cysteine and [<sup>35</sup>S]methionine, and lysed. Lysates were immunoprecipitated with Protein A-Sepharose together with either the S1 domain of the SARS-CoV (TOR2) S protein fused to the Fc domain of human IgG1 (S1-Ig), or with an antibody (1D4) recognizing a tag present at the carboxy-terminus of each of the ACE2 variants, and analyzed by SDS-PAGE. (B) HEK293T cells were transfected with plasmids encoding human ACE2, rat ACE2, or human ACE2 variants in which residues corresponding to those of rat ACE2 were introduced at the indicated position. Transfected cells were analyzed as in (A) and precipitated ACE2 was quantified by phosphorimaging. Values indicate the ratio of protein precipitated by S1-Ig to that precipitated by 1D4. Error bars indicate the range of two or more experiments.

to support infection are localized to the catalytic domain of the receptor.

Guided by the structure of the ACE2 catalytic domain (Towler *et al*, 2004), we made a series of human ACE2 variants in which one or a few solvent-exposed residues were altered to their rat ACE2 counterparts. Two variants consistently bound S1-Ig less efficiently than did wild-type human ACE2. Introduction of rat residues 82–84 (NFS), which include a glycosylation site at asparagine 82 not present in human ACE2, partially inhibited S1-Ig association (Figures 1B and 2A) and S-protein-mediated entry (Figure 2C). Alteration of lysine 353 to a histidine residue present on the rat receptor interfered more dramatically with S1-Ig association, and also partially inhibited S-protein-mediated entry. Introduction of human residues 82–84 (MYP) and lysine 353 into rat ACE2 resulted in substantial

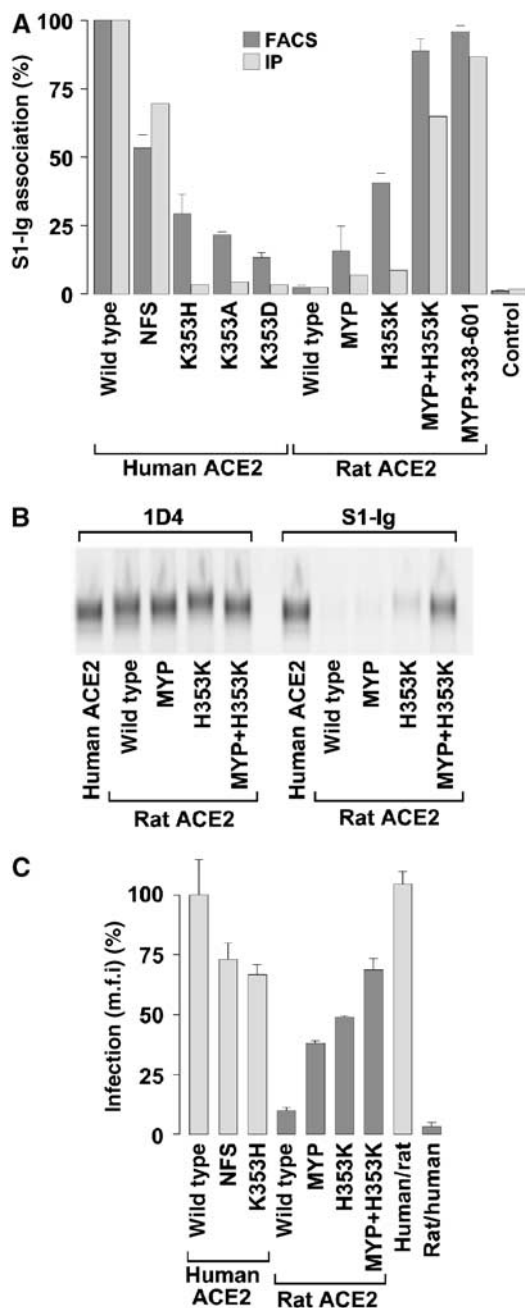


**Figure 2** Introduction of human ACE2 residues into rat ACE2 converts rat ACE2 to an efficient SARS-CoV receptor. (A) HEK293T cells transfected with plasmids encoding the indicated human and rat ACE2 variants or with vector alone were analyzed as in Figure 1 (light gray), or by flow cytometry (dark gray). Flow cytometry values indicate the ratio of mean fluorescence intensity (m.f.i.) observed using S1-Ig to that using the 9E10 antibody, which recognizes a tag present at the amino-terminus of each ACE2 variant. Error bars indicate the range of two or more experiments. (B) Representative example of an immunoprecipitation experiment used in (A). (C) Murine leukemia viruses (MLV) expressing green fluorescent protein (GFP), lacking its endogenous envelope glycoprotein (MLV-GFP), and pseudotyped with the S protein of SARS-CoV (TOR2 isolate) were incubated with HEK293T cells transfected with plasmids encoding the indicated human or rat ACE2 variants. Amount of ACE2-expressing plasmid was adjusted to maintain comparable receptor expression levels, as indicated, by flow cytometry using the antibody 9E10 that recognizes an amino-terminal myc tag on these receptors. GFP expression in cells was quantified by flow cytometry to measure infection of cells by pseudotyped viruses. Error bars indicate range of two experiments.

increases in S1-Ig binding, as assayed both by immunoprecipitation and by flow cytometry (Figure 2A and B). Combination of both sets of residues resulted in a rat ACE2 variant that bound S1-Ig and supported S-protein-mediated infection comparably to human ACE2 (Figure 2A–C). These data suggest that residues 82–84 and, more so, lysine 353 participate in S-protein association with human ACE2.

We subsequently altered a number of additional residues of human ACE2 in the vicinity of residues 82–84 and 353 to alanine or, in some cases, aspartic acid. Alteration of two residues on the first helix of ACE2, at lysine 31 and tyrosine 41, substantially interfered with the S1-Ig association, as did residues adjacent to lysine 353, at aspartic acid 355 and at arginine 357, both within ACE2  $\beta$ -sheet 5 (Figure 3A). Figure 3B–D shows three views of the crystal structure of human ACE2, in which residues that convert rat ACE2 to an efficient SARS-CoV receptor are shown in red, and additional residues whose alteration interferes with S1-Ig association are shown in yellow. Green indicates residues whose alteration did not affect S1-Ig binding. The C-terminal collectrin domain is not well ordered in the structure, but is used here to position the molecule with respect to the cell membrane. As shown in the figures, the S-protein-binding site on ACE2 is localized above the deep cleft that harbors the catalytic site and on the upper left of the structure when viewed facing that cleft.

#### **S-protein association is independent of ACE2 conformational changes**

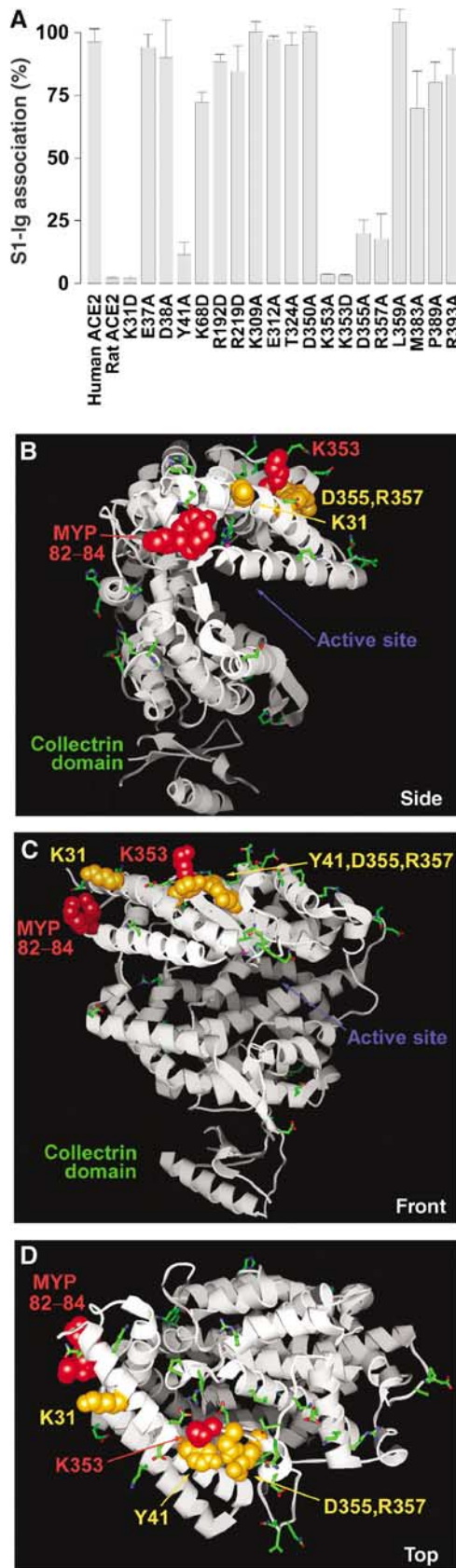
The crystal structure of ACE2 has been solved in two distinct conformations, an open one (Figure 3B–D) and a conformation in which the cleft is closed around the ACE2 inhibitor MLN-4760 (Dales *et al*, 2002; Towler *et al*, 2004). These two conformations likely reflect free and substrate-bound states of the enzyme, respectively. We investigated whether the large conformational change associated with inhibitor binding interfered with S1-Ig binding or S-protein-mediated infection. As previously reported, MLN-4760 inhibits ACE2 activity in the low nanomolar range (Dales *et al*, 2002), and no ACE2 enzymatic activity was detected in the presence of 100 nM inhibitor (Figure 4A). However, 100 nM MLN-4760 did not interfere with immunoprecipitation of ACE2 by S1-Ig, nor did this inhibitor interfere with S-protein-mediated infection (Figure 4B and C). Consistent with these observations, the distances among  $\alpha$  and  $\beta$  carbons of residues 31, 41, 353, 355, and 357 in the S-protein-binding site of ACE2 varied by less than 0.4 Å between the inhibitor-bound and -unbound structures (Towler *et al*, 2004). In contrast, distances between these residues and residues across the cleft typically varied by greater than 6 Å in the two structures. These data suggest that the S-protein-binding region of ACE2 is not perturbed by inhibitors or substrates that induce large conformational changes in the receptor. Consistent with these studies, we have also observed, using the assay shown in Figure 4A, that S1-Ig does not interfere with the enzymatic activity of ACE2 (data not shown).

#### **Association of three S proteins with human and palm-civet ACE2**

The S protein used in the studies above was obtained from a patient infected during the severe 2002–2003 SARS-CoV outbreak. Another outbreak, during the winter of 2003–2004, caused much less severe symptoms in the few individuals

infected and resulted in no documented human-to-human transmissions (He *et al*, 2004; Liang *et al*, 2004; Zhong, 2004; Song *et al*, 2005). We compared an S protein of virus isolated

during this latter outbreak (GD03T0013; accession number AY525636; denoted GD herein) with that of virus obtained during the 2002–2003 outbreak (TOR2; AY274119) and with that isolated from palm civets (SZ3; AY304486) (Guan *et al*, 2003; Marra *et al*, 2003; Rota *et al*, 2003; He *et al*, 2004; Song *et al*, 2005). Figure 5A shows that the S1 domains of all three S proteins efficiently bound palm-civet ACE2 (accession number AY881174), whereas only the S1 domain of TOR2 efficiently bound human ACE2. Of note, the S1 domain of virus isolated during the 2003–2004 outbreak bound palm-civet ACE2 much more efficiently than it bound human ACE2. We then investigated the RBD of each of these S-protein variants. The ability of these S1 domains to bind palm-civet and human ACE2 was reflected in the ability of their respective RBDs to bind these receptors (Figure 5B). We also assayed the ability of the entire S protein to mediate infection of cells expressing human or palm-civet ACE2. The efficiency of entry was consistent with the ability of the S1 domain of each variant to bind each ACE2 (Figure 6C). These data are consistent with the hypothesis that the palm civet is a source of SARS-CoV, and suggest that the apparent lack of severity of disease during the 2003–2004 outbreak may be due in part to incomplete adaptation of GD virus to human ACE2.



### S-protein RBD determinants of association with human ACE2

The RBDs of TOR2 and SZ3 differ by four residues (Figure 6A). We investigated which of these residues contribute to the ability of TOR2 RBD to bind efficiently human ACE2. Each residue in the TOR2 RBD was altered to its SZ3 counterpart. Alteration of two residues, at positions 479 and 487, interfered with the association of the TOR2 RBD with human ACE2 (Figure 6B). Surface plasmon resonance studies further demonstrated a greater than 20-fold decrease of affinity for human ACE2 when either residue 479 or 487, but not when residue 344 or 360, is altered to its palm-civet counterpart (Table I and Supplementary Figure 2). Notably, alteration of threonine 487 to serine also affected the ability of the TOR2 RBD to associate with palm-civet ACE2 (Figure 6B). Introduction of TOR2 residues at 479 or 487 substantially increased the ability of the full SZ3 S protein to infect cells expressing human ACE2. Introduction of SZ3 residues at these positions into the TOR2 S protein resulted in a 2- to 3-fold decrease in infection of these cells

**Figure 3** The S-protein-binding site of human ACE2. (A) Experiments identical to those of Figure 1 except that the indicated solvent-accessible residues common to human and rat ACE2 were modified in human ACE2 to either alanine or aspartic acid. (B) Representation of the crystal structure of human ACE2, with the collectrin domain oriented downward and viewed from the side of the cleft bearing the enzymatic active site. Residues of rat ACE2 whose alteration to the corresponding human residues converted rat ACE2 to an efficient SARS-CoV receptor are shown in red. Human ACE2 residues whose alteration substantially decreased S1-Ig association are shown in orange. Residues whose alteration did not affect S1-Ig association are shown in green. Low-resolution electron density associated with the collectrin domain is represented by a small  $\beta$ -sheet and  $\alpha$ -helix at the base of the figure. (C) A view identical to that in (B) except that the molecule has been rotated 90° about the vertical axis. (D) A view identical to that in (C) except that the molecule has been rotated 90° about the horizontal axis.

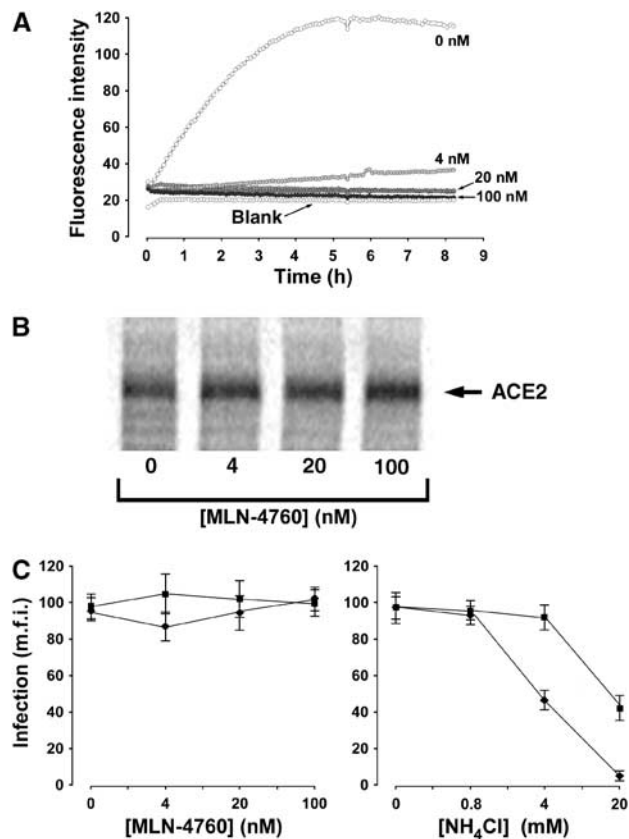


**Figure 4** ACE2 conformational changes induced by an enzymatic inhibitor do not alter S1-Ig association or S-protein-mediated entry. (A) Soluble ACE2 was incubated with a peptide substrate (methoxy-coumarin- YVADAPK(dinitrophenyl)-OH) that fluoresces following cleavage, together with the indicated concentrations of MLN-4760, an inhibitor of ACE2 activity. Fluorescence was measured at 4 min intervals with a fluorescent plate reader. Values indicate average of duplicates. (B) S1-Ig was used to immunoprecipitate ACE2 from lysates of metabolically labeled HEK293T cells transfected with plasmid encoding human ACE2 in the presence of the indicated concentrations of MLN-4760. (C) MLV-GFP virions pseudotyped with the SARS-CoV S protein (diamonds) or with an MLV envelope glycoprotein (squares) were incubated as in Figure 2C with HEK293T cells expressing human ACE2 in the presence of the indicated concentrations of MLN-4760 or NH<sub>4</sub>Cl. Infection as indicated by GFP fluorescence was quantified by flow cytometry. Figures are representative of two experiments with similar results.

(Figure 6C). These data suggest that adaptation of S protein to human ACE2 is facilitated by alteration of residue 479 to asparagine and of 487 to threonine.

#### **Palm-civet and human ACE2 determinants of differential S-protein association**

We also investigated determinants on civet ACE2 that participate in its ability to facilitate efficient infection by GD and SZ3. Two regions within the S-protein-binding site differed significantly between human and palm-civet ACE2 (see Figure 7D and E). A region of  $\alpha$ -helix 1 (residues 30–40) varied at six residues between human and civet ACE2. Likewise, a loop initiating ACE2  $\alpha$ -helix 3 differed by four residues (90–93). A glycosylation site at asparagine 90 of human ACE2 is part of this latter region and is not present in palm-civet ACE2. Figure 7A shows that the S1 domains of GD

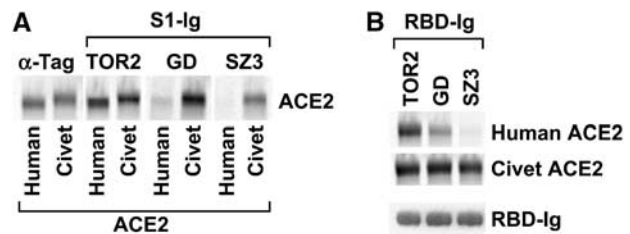


**Figure 5** Differential association of three S proteins with human and palm-civet ACE2. (A) HEK293T cells were transfected with plasmids encoding human or palm-civet ACE2, radiolabeled with [<sup>35</sup>S]cysteine and [<sup>35</sup>S]methionine, and lysed. ACE2 proteins were immunoprecipitated with 1D4, which recognizes a tag present at the carboxy-terminus of each receptor, or with S1-Ig variants containing the S1 domains of TOR2, GD, or SZ3 S proteins, and analyzed by SDS-PAGE. TOR2 SARS-CoV was isolated from humans infected during the 2002–2003 outbreak; GD, during the 2003–2004 outbreak; SZ3, from palm civets. (B) Experiment similar to that in (A) except that S-protein residues 318–510, comprising the RBDs of the indicated S proteins fused to the Fc domain of human IgG1 (RBD-Ig), were used to immunoprecipitate human or palm-civet ACE2. The bottom panel shows a Coomassie-stained SDS-PAGE gel of the individual RBDs used in this experiment.

and SZ3 bound substantially more efficiently when either of these regions was introduced into human ACE2, and that introduction of both regions resulted in receptor binding comparable to that with wild-type palm-civet ACE2. These observations were also reproduced in infection assays (Figure 7B). These data demonstrate that residues within the S-protein-binding domain of ACE2 largely determine the efficiency with which GD and SZ3 S proteins bind and utilize human and palm-civet ACE2.

#### **Binding of RBD chimeras to ACE2 chimeras**

Figure 7C compares the ability of eight RBD variants to bind to human and civet ACE2, as well as to the chimeric molecules assayed in Figure 7A and to a point-mutation variant of palm-civet ACE2, in which aspartic acid 354 was altered to a glycine present in human ACE2. RBD variants were generated from that of TOR2 (left panels) or SZ3 (right panels), and altered at positions 479, 487, or both, as indicated. The panels of Figure 7C permit several conclusions. First, the rough equivalence between the left and right panels indicates that, as implied by Figure 6B and C, S-protein residues 479 and 487 account for most of the differences between TOR2 and SZ3 RBD. Second, no consistent differences were observed between palm-civet ACE2 and its variant with glycine at residue 354, indicating little or no contribution of this residue to S-protein association. Third, consistent with infection data in Figure 6C, the presence of threonine at residue 487 enhanced the affinity of most RBDs for civet and human ACE2, and for variants of these receptors. (Compare, for example, K479/S487 RBD variants with K479/T487 variants for their ability to precipitate each ACE2 variant.) Fourth, and in contrast, substitution of lysine 479 for asparagine in most contexts increased the ability of each RBD variant to associate with human, but not with palm-civet, ACE2. (Compare the binding of N479/T487 RBD with that of K479/T487 variants for binding to human ACE2 (lane 1) and palm-civet ACE2 (lane 6); likewise for N479/S487 and K479/S487 variants.) This enhancement was also observed for ACE2 chimeras containing human  $\alpha$ -helix 1 residues (lanes 1 and 2), but

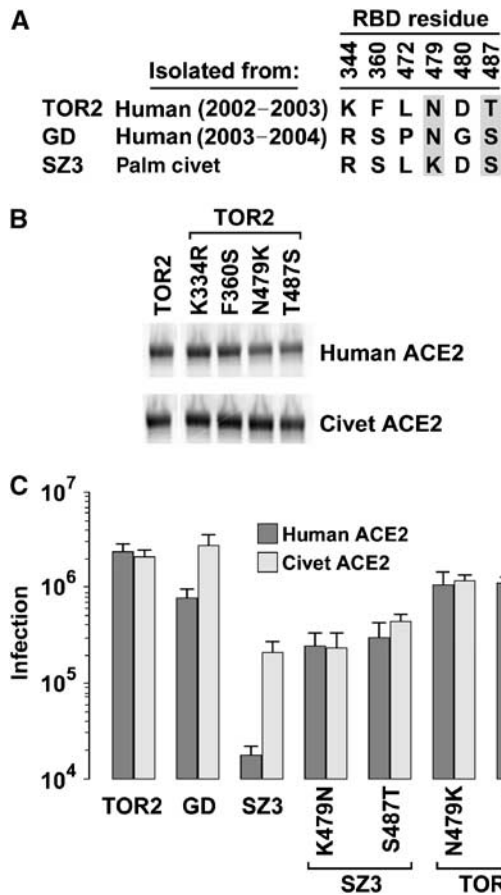


**Figure 6** S-protein RBD determinants of efficient association with human ACE2. (A) Table listing amino-acid differences among the RBDs of the S proteins of the indicated isolates. Residues critical to the differential association of these RBDs with palm-civet and human ACE2 are shown in gray. (B) Experiment similar to that shown in Figure 5B except that individual residues within the TOR2 RBD have been altered to the corresponding residues in the SZ3 RBD. (C) HIV-1-luciferase pseudotyped with S protein of the TOR2, GD, or SZ3 viruses, or with the indicated SZ3 or TOR2 variant, was incubated with HEK293T cells transfected with plasmid encoding human ACE2 or with palm-civet ACE2. Infection, measured as luciferase activity of cell lysates, was assayed 2 days postinfection. The figure shows the mean and range of two experiments.

not those of palm civet (lanes 3, 5, and 6), whereas residues 90–93 did not determine sensitivity to RBD residue 479. Fifth, consistent with infection data in Figure 7B and Supplementary Figure 3, all RBDs bound ACE2 variants bearing residues 90–93 of palm-civet ACE2 substantially more efficiently than they bound equivalent variants with human ACE2 residues at these positions (compare lanes 1 and 2 and lanes 3 and 4 in each panel). Thus, the data of Figure 7C indicate that a lysine at S-protein residue 479 interferes with RBD association with human, but not palm-civet, ACE2. Supplementary Figure 4 shows data consistent with a steric interaction between lysine 31 of human ACE2 and lysine 479 of the SZ3 S protein. Our data also show that alteration of S-protein serine 487 to threonine increases RBD affinity for both human and civet ACE2. Finally, they suggest that no S protein studied has fully adapted to human ACE2 residues 90–93, consistent with a recent zoonotic transmission of the virus.

**Table 1** Kinetics and binding affinity of soluble human ACE2 and RBD-Ig variants

	$k_{on}$ ( $M^{-1} s^{-1}$ )	$k_{off}$ ( $s^{-1}$ )	$K_a$ ( $M^{-1}$ )	$K_d$ (M)
TOR2	$7.12 \times 10^4$	$1.16 \times 10^{-3}$	$6.20 \times 10^7$	$1.62 \times 10^{-8}$
K344R	$6.50 \times 10^4$	$1.04 \times 10^{-3}$	$6.27 \times 10^7$	$1.60 \times 10^{-8}$
F360S	$6.23 \times 10^4$	$8.80 \times 10^{-4}$	$7.08 \times 10^7$	$1.41 \times 10^{-8}$
N479K	$5.73 \times 10^4$	$2.77 \times 10^{-2}$	$2.07 \times 10^6$	$4.84 \times 10^{-7}$
T487S	$3.88 \times 10^4$	$1.37 \times 10^{-2}$	$2.84 \times 10^6$	$3.52 \times 10^{-7}$
SZ3	42.6	$2.35 \times 10^{-2}$	$1.81 \times 10^3$	$5.51 \times 10^{-4}$

Surface plasmon resonance experiments in which the indicated RBD-Ig TOR2 variants shown in Figure 6B bound to immobilized anti-human antibody were assayed for association with soluble human ACE2. The Experiment is representative of two performed with similar results.

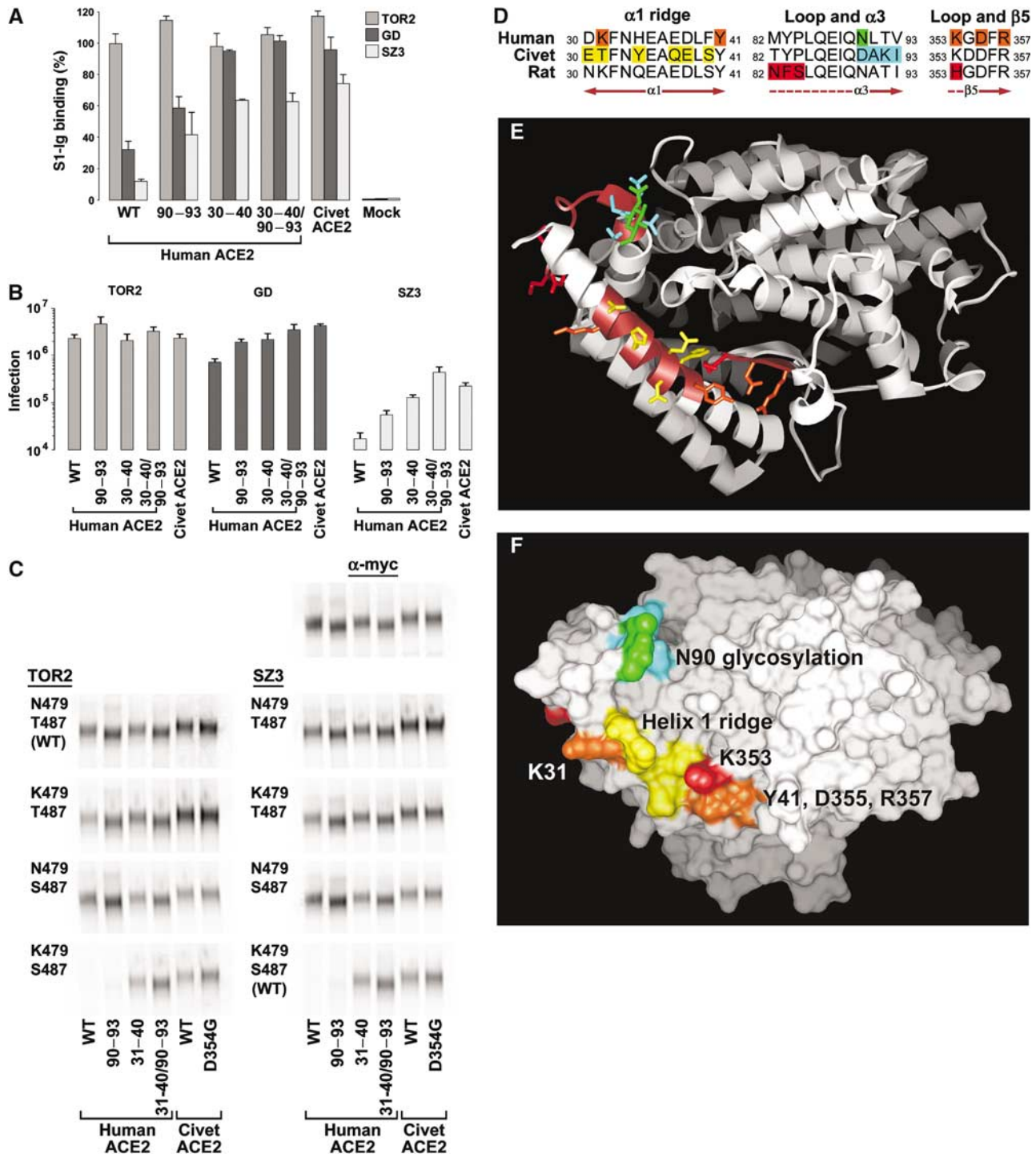
### Mapping determinants to the ACE2 surface

Figure 7D–F summarizes our findings. Figure 7D shows amino-acid sequences of regions critical to S-protein association for palm-civet, rat, and human ACE2. Figure 7E shows ACE2 oriented with the C-terminal membrane-associated collectrin domain facing away from the viewer. Red indicates residues whose alteration transformed rat ACE2 to an efficient SARS-CoV receptor. Orange indicates additional residues common to rat and human ACE2 whose alteration also interferes with S-protein association. Yellow indicates residues along the  $\alpha$ -helix 1 ridge that are unique to palm-civet ACE2, and which permit efficient association with RBD isolates from palm civet and likely interact with lysine 479 of the palm-civet RBD. K31 of human ACE2, which interferes with palm-civet RBD lysine 479, is labeled with white text in Figure 7E. Four residues at the beginning of  $\alpha$ -helix 4 that permit more efficient binding and infection by all S proteins assayed are shown in cyan, and the glycosylation site in this region, present in human but not palm-civet ACE2, is shown in green.

### Discussion

ACE2 is a functional receptor for SARS-CoV, and is likely to play a critical role in viral replication in an infected host (Li *et al*, 2003; Hamming *et al*, 2004; Nie *et al*, 2004). Here we describe the S-protein-binding domain of ACE2. In particular, residues along the first  $\alpha$ -helix, and lysine 353 and proximal residues at the N-terminus of  $\beta$ -sheet 5, participate in S-protein binding and in infection. By altering histidine 353 in rat ACE2 and modifying a glycosylation site that may alter the shape of  $\alpha$ -helix 1, we converted rat ACE2 to an efficient receptor for SARS-CoV. This S-protein-binding region of ACE2 remains intact in the presence of an inhibitor that dramatically alters the overall conformation of ACE2 (Dales *et al*, 2002; Towler *et al*, 2004), consistent with the inability of this inhibitor to block infection, and with the inability of the S protein to modulate ACE2 activity.

Although there can be multiple constraints on interspecies transmission of viruses (Webby *et al*, 2004), S-protein alterations are sufficient to extend or alter the host range of a number of coronaviruses (Kuo *et al*, 2000; Casais *et al*, 2003; Haijema *et al*, 2003; Schickli *et al*, 2004). We have shown that entry is the primary barrier to SARS-CoV infection of murine



**Figure 7** Species-specific ACE2 determinants of differential S-protein association. (A) HEK293T cells transfected with plasmid encoding human or palm-civet ACE2, with human ACE2 bearing the indicated palm-civet residues, or with vector alone were analyzed by flow cytometry using S1-Ig variants of the TOR2, GD, and SZ3 isolates. Error bars indicate the range of two or more experiments. (B) HEK293T cells transfected with plasmid encoding the ACE2 variants used in (A) were incubated with HIV-1-luciferase virus pseudotyped with the S proteins of TOR2, GD, or SZ3 viruses. Infection was assayed as in Figure 6C. (C) HEK293T cells transfected with plasmid encoding human ACE2, human ACE2 variants bearing the indicated palm-civet residues, palm-civet ACE2, or the palm-civet ACE2 variant D354G were metabolically labeled and lysed. Cell lysates were immunoprecipitated with an anti-tag antibody recognizing an amino-terminal tag on these ACE2 variants ( $\alpha$ -myc), or with RBD-Ig of TOR2 or SZ3, or with their variants with the indicated alterations of residues 479 and 487. The experiment is representative of at least two with similar results. (D) Amino-acid content of critical regions of ACE2 from human, palm civet, and rat. Orange indicates human-ACE2 residues whose alteration interferes with TOR2 S-protein association. Red indicates rat-ACE2 residues whose alteration to their human counterparts converts rat ACE2 to an efficient SARS-CoV receptor. Yellow indicates residues of palm-civet ACE2 that accommodate S-protein lysine 479 of SARS-CoV isolated from palm civets. Cyan indicates additional residues of palm-civet ACE2 that, when introduced into human ACE2, result in more efficient association with all S proteins assayed. This effect may be due to the loss of glycosylation at asparagine 90 of human ACE2, shown in green. (E) Ribbon diagram of human ACE2 from the top of the protein. Brown on the ribbon identifies regions shown in (D). Residues highlighted in (D) are shown in the same colors. (F) Surface diagram of human ACE2, from the same orientation as in (E), and colored consistently with (D, E).

cells (Li *et al*, 2004). These observations suggest that S-protein changes may be critical to or sufficient for the adaptation of SARS-CoV to human cells. Accordingly, we compared the S proteins derived from the 2002–2003 outbreak (TOR2), from the less severe 2003–2004 outbreak (GD), and from apparently healthy palm civets (SZ3) (Guan *et al*, 2003; He *et al*, 2004). Strikingly, the receptor-binding regions of each of these S proteins bound palm-civet ACE2 efficiently, but only that from the 2002–2003 outbreak bound human ACE2 with comparable efficiency. These data are consistent with the absence of human-to-human transmission during the 2003–2004 outbreak, and with recent transmission of SARS-CoV from palm civets to humans (Guan *et al*, 2003; Zhong, 2004; Song *et al*, 2005).

Differences among these S proteins permitted identification of key changes necessary for adaptation to the human receptor. In particular, changes at S-protein residues 479 and 487 appear to be critical for high-affinity association with human ACE2. The alteration at 479 to a small, uncharged residue is a consistent property of all described SARS-CoV obtained from humans, whereas most civet-derived viruses retain a basic residue at this position (Guan *et al*, 2003; Marra *et al*, 2003; Rota *et al*, 2003; He *et al*, 2004; Zhang *et al*, 2004; Song *et al*, 2005). Our data indicate that residue 479 interacts with residues along a ridge formed by ACE2  $\alpha$ -helix 1, and in particular with lysine 31, which is present in human but not palm-civet ACE2. Alteration of S-protein residue 479 to the asparagine found in virus isolated from humans appears to accommodate this human ACE2 lysine.

Differences at S-protein residue 487 are also of interest. A threonine at position 487 is absolutely conserved in all of the more than 100 S proteins isolated during the severe 2002–2003 outbreak. In contrast, the S proteins of viruses isolated during the 2003–2004 outbreak, and all 14 animal SARS-CoV isolated, had a serine at this position (Guan *et al*, 2003; He *et al*, 2004; Zhang *et al*, 2004; Song *et al*, 2005). A threonine at position 487 increased affinity of most RBDs assayed for both human and palm-civet ACE2, and all chimeras thereof, and substantially enhanced the efficiency with which palm-civet-derived S protein infected cells expressing human ACE2. These observations indicate that the additional methyl group of threonine 487 participates in the efficiency of infection of human and non-human cells.

S-protein alterations at residues 479 and 487 are important for high-affinity association with human ACE2, and for efficient infection of cells expressing this receptor. Knowledge of these residues may be useful in assessing the risk posed by any new SARS-CoV outbreak. Our data also show that, even with these and other changes outside the RBD, SARS-CoV is imperfectly adapted to its human receptor. In particular, introduction of residues 90–93 of civet ACE2 into the human receptor increased binding of, and infection mediated by, all S proteins assayed. This effect may be due to removal of a glycosylation site at position 90 to which no SARS-CoV has fully adapted. This observation raises the possibility that soluble human ACE2 lacking this glycosylation would more effectively inhibit SARS-CoV replication than wild-type human ACE2.

We have previously shown that replication of SARS-CoV in a murine cell line is limited by the low affinity of the S protein for murine ACE2 (Li *et al*, 2004). Moreover, the affinity of S protein for the receptors of rats, mice, and humans correlates

with the ability of virus to replicate in these animals. The lower affinity of palm-civet-derived S protein for the palm-civet receptor is consistent with this pattern in that no overt disease was manifest in animals from which this virus was isolated (Guan *et al*, 2003), but disease was observed in palm civets challenged with isolates obtained during the 2002–2003 outbreak (Wu *et al*, 2005). Together, these observations suggest that the affinity of S protein for ACE2 is an important determinant in the overall rate of viral replication and in the severity of disease. If so, adaptations within the S protein that are critical for high-affinity association with human ACE2 may have contributed to the unusual severity of SARS.

## Materials and methods

### Construction of S-protein and ACE2 variants

Plasmid encoding a codon-optimized form of the SARS-CoV S protein of the TOR2 isolate (accession number AY274119) has been previously described (Li *et al*, 2003; Moore *et al*, 2004). Plasmids encoding the corresponding S proteins of the GD03T0013 isolate, isolated during the mild 2003–2004 outbreak (accession number AY525636; denoted GD herein), and the SZ3 isolate, isolated from palm civets (accession number AY304486), were generated *de novo* by recursive PCR. Plasmids encoding the S1 domain (residues 12–672) and the RBD (residues 318–510) of the TOR2 S protein, fused to the Fc domain of human IgG1 (S1-Ig and RBD-Ig, respectively), have been previously described (Li *et al*, 2003; Wong *et al*, 2004). Corresponding S1-Ig and RBD-Ig variants of the GD and SZ3 isolates and variant ACE2 molecules were generated by mutagenesis using the QuikChange method (Invitrogen). Human, rat, and palm-civet ACE2 molecules were amplified from cDNA of corresponding tissue by PCR, and cloned into a vector encoding previously described amino- and carboxy-terminal tags (Li *et al*, 2004).

### Binding assays

Association of S1-Ig or RBD-Ig with ACE2 variants was determined by flow cytometry and by immunoprecipitation. Flow cytometry using ACE2-expressing cells has been previously described (Li *et al*, 2003; Wong *et al*, 2004). Briefly, HEK293T cells were transfected with a plasmid encoding ACE2 variants, or with vector alone. At 2 days post-transfection, cells were detached in PBS/5 mM EDTA and washed with PBS/0.5% BSA. S1-Ig or RBD-Ig, or variants thereof, or the anti-tag antibody 9E10, were added to  $10^6$  cells, and the mixture was incubated on ice for 1 h. Cells were washed three times with PBS/0.5% BSA, and then incubated for 30 min on ice with anti-human IgG FITC conjugate (Sigma). Cells were again washed with PBS/0.5% BSA, and analyzed.

Immunoprecipitations were performed as previously described (Li *et al*, 2003; Wong *et al*, 2004). Briefly, HEK293T cells were transfected with plasmid encoding ACE2 variants and radiolabeled with [ $^{35}$ S]cysteine and [ $^{35}$ S]methionine. After 2 days, transfected cells were harvested and lysed in PBS buffer containing 1% CHAPSO. Cell lysates were incubated with Protein A-Sepharose beads together with 2  $\mu$ g S1-Ig or RBD-Ig variants, or with the antibodies 1D4, recognizing a carboxy-terminal C9 tag on ACE2, or 9E10, recognizing an amino-terminal myc tag. Protein A-Sepharose beads were washed three times in PBS/0.5% CHAPSO, and analyzed by SDS-PAGE. Immunoprecipitated ACE2 variants were quantified by phosphorimaging.

TOR2 RBD-Ig variants were also assayed by surface plasmon resonance using a Biacore 3000. A 200 nM portion of purified RBD-Ig of TOR2 variants was bound to an anti-human antibody (Sigma I-2136) immobilized on a CM5 sensor chip. Soluble human ACE2 in HBS-EP buffer (Biacore) was introduced at a flow rate of 20  $\mu$ l/min at concentrations of 700, 200, 40, 8, 1.6, and 0 nM. Kinetic parameters were determined with BIA-EVALUATION software (Biacore).

### Infection with S-protein-pseudotyped retrovirus

MLV expressing GFP and pseudotyped with SARS-CoV S-protein variants has been previously described (Moore *et al*, 2004). Briefly, MLV virions were generated by cotransfecting plasmid encoding

MLV *gag* and *pol* genes, the pQCXIX vector (BD Sciences) expressing GFP, and plasmid encoding S-protein variants. At 48 h post-transfection, cell supernatants were normalized for reverse transcriptase activity and incubated with HEK293T cells transfected with ACE2 variants. At 48 h postincubation, GFP fluorescence of infected cells was measured by flow cytometry. In some cases, cells were preincubated for 1 h with the ACE2 inhibitor MLN-4760 or with NH<sub>4</sub>Cl before infection, and equivalent concentrations were maintained during infection.

Infection was also assayed with a lentivirus expressing a luciferase reporter gene and pseudotyped with S-protein variants, as previously described (Sui *et al*, 2005). Briefly, 293T cells were cotransfected with plasmid encoding S-protein variants, a plasmid (pCMVΔR8.2) encoding HIV-1 Gag-Pol, and a plasmid (pHIV-Luc) encoding the firefly luciferase reporter gene under control of the HIV-1 long terminal repeat. At 2 days post-transfection, viral supernatants were harvested and 3 μl of S-protein-pseudotyped virus was used for infection of 6000 ACE2-expressing 293T cells in a 96-

well plate. Infection efficiency was quantitated by measuring the luciferase activity in the target cells with an EG&G Berthold Microplate Luminometer LB 96V.

#### ACE2 enzymatic activity

The enzymatic activity of ACE2 was assayed using a fluorogenic substrate, 7-methoxycoumarin-YVADAPK(2,4-dinitrophenyl)-OH (R&D Systems). Cleavage of this peptide by ACE2 removes the 2,4-dinitrophenyl moiety that quenches the fluorescence of the 7-methoxycoumarin moiety. A 1 μg portion of a soluble form of ACE2 (Moore *et al*, 2004) was incubated in 100 mM Tris buffer with varying concentrations of the ACE2 inhibitor MLN-4760 (Dales *et al*, 2002). Fluorescence was monitored at 5 min intervals using an excitation wavelength of 330 nm and emission wavelength of 450 nm.

#### Supplementary data

Supplementary data are available at *The EMBO Journal* Online.

## References

- Babcock GJ, Eshaki DJ, Thomas Jr WD, Ambrosino DM (2004) Amino acids 270 to 510 of the severe acute respiratory syndrome coronavirus spike protein are required for interaction with receptor. *J Virol* **78**: 4552–4560
- Casas R, Dove B, Cavanagh D, Britton P (2003) Recombinant avian infectious bronchitis virus expressing a heterologous spike gene demonstrates that the spike protein is a determinant of cell tropism. *J Virol* **77**: 9084–9089
- Chan PK, To KF, Lo AW, Cheung JL, Chu I, Au FW, Tong JH, Tam JS, Sung JJ, Ng HK (2004) Persistent infection of SARS coronavirus in colonic cells *in vitro*. *J Med Virol* **74**: 1–7
- Dales NA, Gould AE, Brown JA, Calderwood EF, Guan B, Minor CA, Gavin JM, Hales P, Kaushik VK, Stewart M, Tummino PJ, Vickers CS, Ocain TD, Patane MA (2002) Substrate-based design of the first class of angiotensin-converting enzyme-related carboxypeptidase (ACE2) inhibitors. *J Am Chem Soc* **124**: 11852–11853
- Ding Y, He L, Zhang Q, Huang Z, Che X, Hou J, Wang H, Shen H, Qiu L, Li Z, Geng J, Cai J, Han H, Li X, Kang W, Weng D, Liang P, Jiang S (2004) Organ distribution of severe acute respiratory syndrome (SARS) associated coronavirus (SARS-CoV) in SARS patients: implications for pathogenesis and virus transmission pathways. *J Pathol* **203**: 622–630
- Drosten C, Gunther S, Preiser W, van der Werf S, Brodt HR, Becker S, Rabenau H, Panning M, Kolesnikova L, Fouchier RA, Berger A, Burguiere AM, Cinatl J, Eickmann M, Escriou N, Grywna K, Kramme S, Manuguerra JC, Muller S, Rickerts V, Sturmer M, Vieth S, Klenk HD, Osterhaus AD, Schmitz H, Doerr HW (2003) Identification of a novel coronavirus in patients with severe acute respiratory syndrome. *N Engl J Med* **348**: 1967–1976
- Fouchier RA, Kuiken T, Schutten M, van Amerongen G, van Doornum GJ, van den Hoogen BG, Peiris M, Lim W, Stohr K, Osterhaus AD (2003) Aetiology: Koch's postulates fulfilled for SARS virus. *Nature* **423**: 240
- Gallagher TM, Buchmeier MJ (2001) Coronavirus spike proteins in viral entry and pathogenesis. *Virology* **279**: 371–374
- Guan Y, Zheng BJ, He YQ, Liu XL, Zhuang ZX, Cheung CL, Luo SW, Li PH, Zhang LJ, Guan YJ, Butt KM, Wong KL, Chan KW, Lim W, Shorridge KF, Yuen KY, Peiris JS, Poon LL (2003) Isolation and characterization of viruses related to the SARS coronavirus from animals in Southern China. *Science* **4**: 4
- Haijema BJ, Volders H, Rottier PJ (2003) Switching species tropism: an effective way to manipulate the feline coronavirus genome. *J Virol* **77**: 4528–4538
- Hamming I, Timens W, Bultuis ML, Lely AT, Navis GJ, van Goor H (2004) Tissue distribution of ACE2 protein, the functional receptor for SARS coronavirus. A first step in understanding SARS pathogenesis. *J Pathol* **203**: 631–637
- Harmer D, Gilbert M, Borman R, Clark KL (2002) Quantitative mRNA expression profiling of ACE 2, a novel homologue of angiotensin converting enzyme. *FEBS Lett* **532**: 107–110
- He JF, Peng GW, Min J, Yu DW, Liang WJ, Zhang SY, Xu RH, Zheng HY, Wu XW, Xu J, Wang ZH, Fang L, Zhang X, Li H, Yan XG, Lu JH, Hu ZH, Huang JC, Wan XW (2004) Molecular evolution of the SARS coronavirus during the course of the SARS epidemic in China. *Science* **303**: 1666–1669, Epub 2004 Jan 29
- Hofmann H, Geier M, Marzi A, Krumbiegel M, Peipp M, Fey GH, Gramberg T, Pohlmann S (2004) Susceptibility to SARS coronavirus S protein-driven infection correlates with expression of angiotensin converting enzyme 2 and infection can be blocked by soluble receptor. *Biochem Biophys Res Commun* **319**: 1216–1221
- Hofmann H, Pohlmann S (2004) Cellular entry of the SARS coronavirus. *Trends Microbiol* **12**: 466–472
- Holmes KV (2003) SARS-associated coronavirus. *N Engl J Med* **348**: 1948–1951
- Jeffers SA, Tusell SM, Gillim-Ross L, Hemmila EM, Achenbach JE, Babcock GJ, Thomas Jr WD, Thackray LB, Young MD, Mason RJ, Ambrosino DM, Wentworth DE, Demartini JC, Holmes KV (2004) CD209L (L-SIGN) is a receptor for severe acute respiratory syndrome coronavirus. *Proc Natl Acad Sci USA* **101**: 15748–15753, Epub 2004 Oct 20
- Ksiazek TG, Erdman D, Goldsmith CS, Zaki SR, Peret T, Emery S, Tong S, Urbani C, Comer JA, Lim W, Rollin PE, Dowell SF, Ling AE, Humphrey CD, Shieh WJ, Guarner J, Paddock CD, Rota P, Fields B, DeRisi J, Yang JY, Cox N, Hughes JM, LeDuc JW, Bellini WJ, Anderson LJ (2003) A novel coronavirus associated with severe acute respiratory syndrome. *N Engl J Med* **348**: 1953–1966
- Kuiken T, Fouchier RA, Schutten M, Rimmelzwaan GF, van Amerongen G, van Riel D, Laman JD, de Jong T, van Doornum G, Lim W, Ling AE, Chan PK, Tam JS, Zambon MC, Gopal R, Drosten C, van der Werf S, Escriou N, Manuguerra JC, Stohr K, Peiris JS, Osterhaus AD (2003) Newly discovered coronavirus as the primary cause of severe acute respiratory syndrome. *Lancet* **362**: 263–270
- Kuo L, Godeke GJ, Raamsman MJ, Masters PS, Rottier PJ (2000) Retargeting of coronavirus by substitution of the spike glycoprotein ectodomain: crossing the host cell species barrier. *J Virol* **74**: 1393–1406
- Li W, Greenough TC, Moore MJ, Vasilieva N, Somasundaran M, Sullivan JL, Farzan M, Choe H (2004) Efficient replication of severe acute respiratory syndrome coronavirus in mouse cells is limited by murine angiotensin-converting enzyme 2. *J Virol* **78**: 11429–11433
- Li W, Moore MJ, Vasilieva N, Sui J, Wong SK, Berne MA, Somasundaran M, Sullivan JL, Luzeriyaga C, Greenough TC, Choe H, Farzan M (2003) Angiotensin-converting enzyme 2 is a functional receptor for the SARS coronavirus. *Nature* **426**: 450–454
- Liang G, Chen Q, Xu J, Liu Y, Lim W, Peiris JS, Anderson LJ, Ruan L, Li H, Kan B, Di B, Cheng P, Chan KH, Erdman D, Gu S, Xinge Y, Liang W, Zhou D, Haynes L (2004) Laboratory diagnosis of four recent sporadic cases of community-acquired SARS, Guangdong Province, China. *Emerg Infect Dis* **10**: 1774–1781
- Marra MA, Jones SJ, Astell CR, Holt RA, Brooks-Wilson A, Butterfield YS, Khattri J, Asano JK, Barber SA, Chan SY, Cloutier A, Coughlin SM, Freeman D, Girn N, Griffith OL, Leach SR, Mayo M, McDonald H, Montgomery SB, Pandoh PK, Petrescu AS, Robertson AG,

- Schein JE, Siddiqui A, Smailus DE, Stott JM, Yang GS, Plummer F, Andonov A, Artsob H, Bastien N, Bernard K, Booth TF, Bowness D, Czub M, Drebot M, Fernando L, Flick R, Garbutt M, Gray M, Grolla A, Jones S, Feldmann H, Meyers A, Kabani A, Li Y, Normand S, Stroher U, Tipples GA, Tyler S, Vogrig R, Ward D, Watson B, Brunham RC, Kraiden M, Petric M, Skowronski DM, Upton C, Roper RL (2003) The genome sequence of the SARS-associated coronavirus. *Science* **300**: 1399–1404
- Marzi A, Gramberg T, Simmons G, Moller P, Rennekamp AJ, Krumbiegel M, Geier M, Eisemann J, Turza N, Saunier B, Steinkasserer A, Becker S, Bates P, Hofmann H, Pohlmann S (2004) DC-SIGN and DC-SIGNR interact with the glycoprotein of Marburg virus and the S protein of severe acute respiratory syndrome coronavirus. *J Virol* **78**: 12090–12095
- Moore MJ, Dorfman T, Li W, Wong SK, Li Y, Kuhn JH, Coderre J, Vasilieva N, Han Z, Greenough TC, Farzan M, Choe H (2004) Retroviruses pseudotyped with the severe acute respiratory syndrome coronavirus spike protein efficiently infect cells expressing angiotensin-converting enzyme 2. *J Virol* **78**: 10628–10635
- Nie Y, Wang P, Shi X, Wang G, Chen J, Zheng A, Wang W, Wang Z, Qu X, Luo M, Tan L, Song X, Yin X, Ding M, Deng H (2004) Highly infectious SARS-CoV pseudotyped virus reveals the cell tropism and its correlation with receptor expression. *Biochem Biophys Res Commun* **321**: 994–1000
- Normile D (2004) Infectious diseases. Mounting lab accidents raise SARS fears. *Science* **304**: 659–661
- Peiris JS, Guan Y, Yuen KY (2004) Severe acute respiratory syndrome. *Nat Med* **10**: S88–97
- Rota PA, Oberste MS, Monroe SS, Nix WA, Campagnoli R, Icenogle JP, Penaranda S, Bankamp B, Maher K, Chen MH, Tong S, Tamin A, Lowe L, Frace M, DeRisi JL, Chen Q, Wang D, Erdman DD, Peret TC, Burns C, Ksiazek TG, Rollin PE, Sanchez A, Liffick S, Holloway B, Limor J, McCaustland K, Olsen-Rasmussen M, Fouchier R, Gunther S, Osterhaus AD, Drosten C, Pallansch MA, Anderson LJ, Bellini WJ (2003) Characterization of a novel coronavirus associated with severe acute respiratory syndrome. *Science* **300**: 1394–1399
- Schickli JH, Thackray LB, Sawicki SG, Holmes KV (2004) The N-terminal region of the murine coronavirus spike glycoprotein is associated with the extended host range of viruses from persistently infected murine cells. *J Virol* **78**: 9073–9083
- Song HD, Tu CC, Zhang GW, Wang SY, Zheng K, Lei LC, Chen QX, Gao YW, Zhou HQ, Xiang H, Zheng HJ, Chern SW, Cheng F, Pan CM, Xuan H, Chen SJ, Luo HM, Zhou DH, Liu YF, He JF, Qin PZ, Li LH, Ren YQ, Liang WJ, Yu YD, Anderson L, Wang M, Xu RH, Wu XW, Zheng HY, Chen JD, Liang G, Gao Y, Liao M, Fang L, Jiang LY, Li H, Chen F, Di B, He LJ, Lin JY, Tong S, Kong X, Du L, Hao P, Tang H, Bernini A, Yu XJ, Spiga O, Guo ZM, Pan HY, He WZ, Manuguerra JC, Fontanet A, Danchin A, Niccolai N, Li YX, Wu CI, Zhao GP (2005) Cross-host evolution of severe acute respiratory syndrome coronavirus in palm civet and human. *Proc Natl Acad Sci USA* **102**: 2430–2435, Epub 2005 Feb 04
- Subbarao K, McAuliffe J, Vogel L, Fahle G, Fischer S, Tatti K, Packard M, Shieh WJ, Zaki S, Murphy B (2004) Prior infection and passive transfer of neutralizing antibody prevent replication of severe acute respiratory syndrome coronavirus in the respiratory tract of mice. *J Virol* **78**: 3572–3577
- Sui J, Li W, Murakami A, Tamin A, Matthews LJ, Wong SK, Moore MJ, St Clair Tallarico A, Olurinde M, Choe H, Anderson LJ, Bellini WJ, Farzan M, Marasco WA (2004) Potent neutralization of severe acute respiratory syndrome (SARS) coronavirus by a human mAb to S1 protein that blocks receptor association. *Proc Natl Acad Sci USA* **101**: 2536–2541
- Sui J, Li W, Roberts A, Matthews LJ, Murakami A, Vogel L, Wong SK, Subbarao K, Farzan M, Marasco WA (2005) Evaluation of human mAb 80R in immunoprophylaxis of SARS by an animal study, epitope mapping and analysis of spike variants. *J Virol* in press
- Towler P, Staker B, Prasad SG, Menon S, Tang J, Parsons T, Ryan D, Fisher M, Williams D, Dales NA, Patane MA, Pantoliano MW (2004) ACE2 X-ray structures reveal a large hinge-bending motion important for inhibitor binding and catalysis. *J Biol Chem* **279**: 17996–18007, Epub 2004 Jan 30
- Webby R, Hoffmann E, Webster R (2004) Molecular constraints to interspecies transmission of viral pathogens. *Nat Med* **10**: S77–S81
- Wentworth DE, Gillim-Ross L, Espina N, Bernard KA (2004) Mice susceptible to SARS coronavirus. *Emerg Infect Dis* **10**: 1293–1296
- Wong SK, Li W, Moore MJ, Choe H, Farzan M (2004) A 193-amino acid fragment of the SARS coronavirus S protein efficiently binds angiotensin-converting enzyme 2. *J Biol Chem* **279**: 3197–3201, Epub 2003 Dec 11
- Wu D, Tu C, Xin C, Xuan H, Meng Q, Liu Y, Yu Y, Guan Y, Jiang Y, Yin X, Cramer G, Wang M, Li C, Liu S, Liao M, Feng L, Xiang H, Sun J, Chen J, Sun Y, Gu S, Liu N, Fu D, Eaton BT, Wang LF, Kong X (2005) Civets are equally susceptible to experimental infection by two different severe acute respiratory syndrome coronavirus isolates. *J Virol* **79**: 2620–2625
- Xiao X, Chakraborti S, Dimitrov AS, Gramatikoff K, Dimitrov DS (2003) The SARS-CoV S glycoprotein: expression and functional characterization. *Biochem Biophys Res Commun* **312**: 1159–1164
- Yang ZY, Huang Y, Ganesh L, Leung K, Kong WP, Schwartz O, Subbarao K, Nabel GJ (2004) pH-dependent entry of severe acute respiratory syndrome coronavirus is mediated by the spike glycoprotein and enhanced by dendritic cell transfer through DC-SIGN. *J Virol* **78**: 5642–5650
- Zhang H, Wada J, Hida K, Tsuchiyama Y, Hiragushi K, Shikata K, Wang H, Lin S, Kanwar YS, Makino H (2001) Collectrin, a collecting duct-specific transmembrane glycoprotein, is a novel homolog of ACE2 and is developmentally regulated in embryonic kidneys. *J Biol Chem* **276**: 17132–17139
- Zhang Y, Zheng N, Hao P, Zhong Y (2004) Reconstruction of the most recent common ancestor sequences of SARS-CoV S gene and detection of adaptive evolution in the spike protein. *Chinese Sci Bull* **49**: 1311–1313
- Zhong N (2004) Management and prevention of SARS in China. *Philos Trans R Soc London B* **359**: 1115–1116